

Synthesis, Thermoanalysis, and Thermal Kinetic Thermogravimetric Analysis of Transition Metal Co(II), Ni(II), Cu(II), and Zn(II) Complexes with 2-(2-Hydroxyphenyl)benzimidazole (HL)

Min Jiang,[‡] Jun Li,^{*,†} Yong-qian Huo,[§] Yun Xi,[†] Jun-feng Yan,[†] and Feng-xing Zhang[†]

[†]Key Laboratory of Synthetic and Natural Functional Molecule Chemistry of Ministry of Education, College of Chemistry & Materials Science, Northwest University, Xian, Shaanxi 710069, China

[‡]School of Chemistry and Environment Science, Shaanxi University of Technology, Hanzhong, Shaanxi, 723000, China

[§]College of Chemistry & Chemistry Engineering, Yanan University, Yan'an, Shaanxi, 716000, China

ABSTRACT: Four complexes with general formulas $M^{II}L_2 \cdot CH_3OH$ ($M = Co, Zn$) and $M^{II}L_2$ ($M = Ni, Cu$) were synthesized by transition metal ions M^{II} (Co, Ni, Cu, Zn) reacting with 2-(2-hydroxyphenyl)benzimidazole (HL). Their thermal properties were studied; the probable thermal decomposition mechanism for the first step of the Co(II) and Zn(II) complexes was suggested, and the kinetic parameters were also given.

1. INTRODUCTION

The fluorescent compound 2-(2-hydroxyphenyl)benzimidazole (HPBI) (Figure 1) is useful as a laser dye, high energy radiation detector, molecular energy storage system, and fluorescent probe.^{1–3} The excited state intramolecular proton transfer mechanism about it and its analogues have been extensively studied,^{4–7} which showed a high Stokes shift and a great thermal and photophysical stability.

The bidentate ligand HPBI is structurally similar to N-substituted salicylaldehydes, which have been widely used in transition metal coordination chemistry. Moreover, HPBI comprises two groups of relevance to the coordination of metal centers in biological systems, namely, phenolate (tyrosine) and imidazole (histidine). In the past, some metal complexes with HPBI derivatives have been synthesized and structurally characterized by other groups^{8–13} and by us,^{14–16} and some of them displayed good photoluminescence and magnetic properties. However, the thermal stability and decomposition steps of these complexes have been rarely reported.

In this paper, four complexes of HPBI with divalent transition metal ions M^{II} (Co, Ni, Cu, Zn) were prepared, with general formula $M^{II}L_2 \cdot CH_3OH$ ($M = Co, Zn$) and $M^{II}L_2$ ($M = Ni, Cu$), and the thermal properties of these complexes were studied. To the complexes of $CoL_2 \cdot CH_3OH$ and $ZnL_2 \cdot CH_3OH$, the kinetics mechanism of the first-step decomposition reaction is also reported.

2. EXPERIMENTAL SECTION

2.1. Materials and Methods. $CoCl_2 \cdot 6H_2O$, $NiCl_2 \cdot 6H_2O$, $CuCl_2 \cdot 2H_2O$, $ZnCl_2$, methanol, ethanol, KOH, salicylaldehyde, and *o*-phenylenediamine were all analytical reagent or guaranteed reagent grade from China. Elemental analyses (C, H, and N) were performed by a Vario EL-CHNOS instrument. The metal content in the complexes was determined, after destroying the organic matter with aqua regia and then with concentrated

sulfuric acid, by ethylenediaminetetraacetic (EDTA) titrations. Molar conductance measurements were made with a DDS-307 conductivity meter. IR spectra were obtained with a Bruker EQ UINOX-550 spectrophotometer in the region of (4000 to 400) cm^{-1} . The thermoanalysis curves were obtained using a NETZCH STA449C thermal analysis instrument. The atmosphere was nitrogen, with a flow rate of $30 mL \cdot min^{-1}$. The rate of heating was (15, 10, or 5) $^{\circ}C \cdot min^{-1}$, and the sensitivity of the instrument is 0.1 μg . The sample mass is (2 to 4) mg. The thermal kinetic thermogravimetric (TG) analysis adopted the kinetic software from NETZSCH.

2.2. Synthesis of 2-(2-Hydroxyphenyl)benzimidazole (HL). A solution of 2.32 g (19 mmol) of salicylaldehyde in 15 mL EtOH was added to a solution of 2.05 g (19 mmol) of *o*-phenylenediamine in 25 mL of EtOH under stirring and heating. The resulting orange solution was refluxed for 1 h and then cooled to room temperature. After 12 h in the refrigerator, the orange solution was filtered, and 15 mL of ether was added to the solution. The solution was placed in the open air for 2 days; some needle orange crystals appeared. The crystals were filtered and then air-dried. The yield was 52 % and melting point (251 to 252) $^{\circ}C$.

2.3. Synthesis of the Complexes. The HL (0.420 g, 2.0 mmol) and KOH (0.112 g, 2.0 mmol) were dissolved in a sufficient amount of methanol, and then $CoCl_2 \cdot 6H_2O$ (0.238 g, 1.0 mmol) in 20 mL methanol was added to this solution with stirring. The product began to crystallize from the solution almost immediately. After 1 h at room temperature, the solid was filtered off, washed with methanol, and air-dried. The yield was 76 %.

Special Issue: John M. Prausnitz Festschrift

Received: October 26, 2010

Accepted: January 24, 2011

Published: February 10, 2011

The syntheses of the Ni, Cu, and Zn complexes are similar to that of the Co complex, and the metal salts are $\text{NiCl}_2 \cdot 6\text{H}_2\text{O}$, $\text{CuCl}_2 \cdot 2\text{H}_2\text{O}$, and ZnCl_2 , respectively. Yields: 58 % (Ni), 83 % (Cu), and 70 % (Zn).

2.4. Theory Base of the Kinetics Estimation of the Thermal Decomposition. According to nonisothermal kinetic models, the differential and integral forms of a rate equation are generally expressed, as follows:

$$\frac{d\alpha}{dT} = \frac{A}{\beta} f(\alpha) \exp\left(\frac{-E_a}{RT}\right) \quad (1)$$

$$g(\alpha) = \frac{AE}{\beta R} p(x) \quad (2)$$

where $x = E/RT$, E is the activation energy, A the pre-exponential factor, R the gas constant, α the degree of conversion, $\beta = dT/dt$ the heating rate, $g(\alpha)$ and $f(\alpha)$ are appropriate functions of α , and $p(x)$ represents the integral

$$\int_x^\infty \frac{\exp(-x)}{x^2} dx \quad (3)$$

A difficulty in nonisothermal kinetic methods is that there is no exact analytical solution of the $p(x)$ function. Doyle¹⁷ has suggested that $\log p(x)$ is an approximately linear function of x , that is, of $1/T$.

$$\log p(x) = -2.315 - 0.4567x \quad (4)$$

However, Vyazovkin and Dollimore¹⁸ has considered that the application is restricted ($x > 13$).

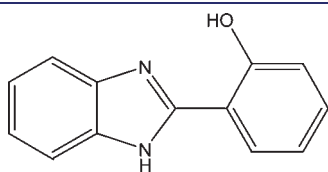


Figure 1. Structure of 2-(2-hydroxyphenyl)benzimidazole (HPBI).

The lack of knowledge of the analytical form of $g(\alpha)$ can be circumvented quite easily by combining eqs 2 and 4:

$$\log \beta = -0.4567 \frac{E}{RT} + \text{constant} \quad (5)$$

For a number of experiments with different temperature programs, β , we can write for the same extent of reaction α

$$\log \beta = \log \frac{AE}{Rg(\alpha)} - 2.315 - 0.4567 \frac{E}{RT} \quad (6)$$

The plot of $\log \beta$ versus $1/T$ for a given value of α must give the activation energy E . The procedure was suggested by both Ozawa¹⁹ and Flynn and Wall.²⁰ We can use the method for determining E which does not depend on a knowledge of the analytical form of $g(\alpha)$.

Another method is the ASTM E698.²¹ It uses a model-free estimate for E which is evaluated from Kissinger's plot of $\ln(\beta/T_m^2)$ against T_m^{-1} ,²² where T_m is the temperature corresponding to the maximum of $d\alpha/dT$. However, the pre-exponential factor is evaluated on the assumption of first-order reactions as follows:

$$A = \frac{\beta E}{RT_m^2} \exp\left(\frac{E}{RT_m}\right) \quad (7)$$

The method occupies an intermediate position between the model-fitting and the model-free methods.²³

Using the kinetic software from NETZSCH, the multivariate nonlinear regression method is used to fit the kinetic curves. The 15 mechanism functions applied to describe thermal decomposition in solids are shown in Table 1.

3. RESULTS AND DISCUSSION

3.1. Structural Characterization. The structure of ligand HL is shown in Figure 2a. It is only a fake plane for a very small dihedral angle ($\theta = 2.2^\circ$) which was found between the benzimidazole plane and the phenolate plane. Meanwhile, there is a

Table 1. Selected 15 Mechanism Functions for the Evaluation of the Kinetic Equations

mechanisms	symbol	$f(\alpha)$	$g(\alpha)$
random nucleation; unimolecular decay (first order)	F1	$(1 - \alpha)$	$-\ln(1 - \alpha)$
formal chemical reaction (second order)	F2	$(1 - \alpha)^2$	$(1 - \alpha)^{-1}$
formal chemical reaction (n th order)	F n	$(1 - \alpha)^n$	$[1 - (1 - \alpha)^{1-n}]/(1 - n)$
one-dimensional diffusion (parabola law)	D1	$1/2\alpha^{-1}$	α^2
two-dimensional diffusion (Valensi equation)	D2	$-1/\ln(1 - \alpha)$	$(1 - \alpha)\ln(1 - \alpha) + \alpha$
three-dimensional diffusion (Jander equation)	D3	$3/2(1 - \alpha)^{2/3}[1 - (1 - \alpha)^{1/3}]^{-1}$	$[1 - (1 - \alpha)^{1/3}]^2$
three-dimensional diffusion (Ginst-Broun equation)	D4	$3/2[(1 - \alpha)^{-1/3} - 1]^{-1}$	$(1 - 2\alpha/3) - (1 - \alpha)^{2/3}$
phase boundary reaction (contracting cylinder)	R2	$2(1 - \alpha)^{1/2}$	$1 - (1 - \alpha)^{1/2}$
phase boundary reaction (contracting sphere)	R3	$3(1 - \alpha)^{2/3}$	$1 - (1 - \alpha)^{1/3}$
autocatalysis, ramiform nucleation	B1	$(1 - \alpha)\alpha$	$\ln[\alpha/(1 - \alpha)]$
autocatalysis, ramiform nucleation	B n a	$(1 - \alpha)^n \alpha^a$	
first order with autocatalysis	C1	$(1 - \alpha)(1 + K\alpha)$	
two-dimensional nucleation and growth	A2	$2(1 - \alpha)[- \ln(1 - \alpha)]^{1/2}$	$[- \ln(1 - \alpha)]^{1/2}$
three-dimensional nucleation and growth	A3	$3(1 - \alpha)[- \ln(1 - \alpha)]^{2/3}$	$[- \ln(1 - \alpha)]^{1/3}$
n -dimensional nucleation and growth	A n	$n(1 - \alpha)[- \ln(1 - \alpha)]^{(n-1)/n}$	$[- \ln(1 - \alpha)]^{1/n}$

intramolecular hydrogen bond between the phenolic OH group and the N atom of benzimidazole ring with a corresponding O1...N2 distance of 2.578(2) Å.

Figure 2b displays the one-dimensional zigzag chain structure of HL constructed by intermolecular hydrogen bonding interactions. The imidazole group donates a hydrogen bond to the phenolate O atom of the adjacent molecule [N(1A)...O(1B) 2.909(2) Å], resulting in a one-dimensional zigzag chain. The structure gives proof of the good thermal stability of HL.

The color, molar conductance, and elemental analysis of these complexes are shown in Table 2.

The molar conductivities of these complexes in 0.001 mol·L⁻¹ DMF solutions are in the range of (0.385 to 1.24) S·cm²·mol⁻¹, indicating that these compounds are nonelectrolytes.²⁴ All four metal complexes displayed low solubility in water and common organic solvents except for dimethylformamide (DMF) and dimethyl sulfoxide (DMSO). The bivalent metal ions bond two HL anions in all four complexes. The Co and Zn complexes contain a CH₃OH molecule.

The IR spectra of HL exhibits a strong ν_{N-H} stretching band at 3327 cm⁻¹, and a broad absorption band at (3000 to 2800) cm⁻¹ is attributed to the intramolecular hydrogen bond.²⁵ The (1633, 1266, and 727) cm⁻¹ bands are attributed to the stretching vibration of ν_{C=N}, ν_{C-O}, and the four adjacent H atoms in the phenyl ring, respectively.

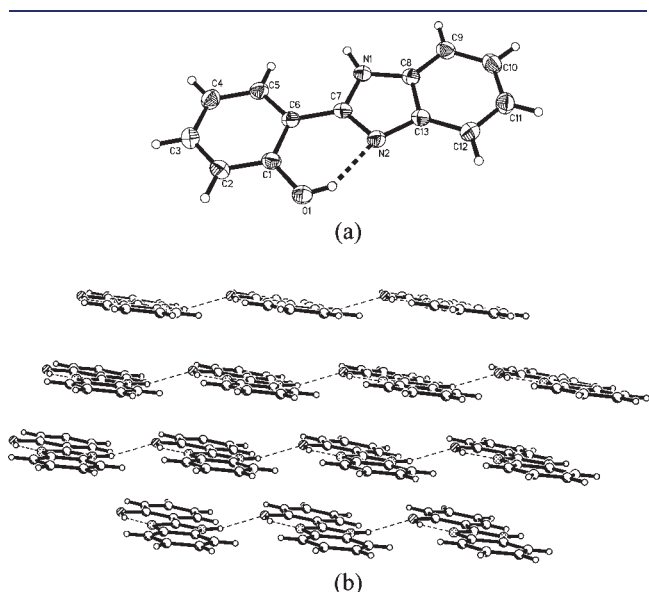


Figure 2. (a) Structure of HL; the dashed line denotes the intramolecular hydrogen bond. (b) One-dimensional zigzag chain of HL formed by intermolecular hydrogen bonds.

The broad absorption bands of ν_{OH} are not observed in the IR spectra of the four complexes, indicating M–O bond formation. There is a shift of the C=N vibration to lower frequencies [(1622 to 1626) cm⁻¹] which is assigned to N-metal coordination. The conclusive evidence of bonding of the oxygen and nitrogen atoms to the metal ions is confirmed by the appearance of bands at ~435 cm⁻¹ and ~470 cm⁻¹ in all four complexes which are assigned to ν_(M-O) and ν_(M-N) vibrations, respectively. A new band at ~1030 cm⁻¹ can be found in the IR spectra of the Co(II) and Zn(II) complexes, which is assigned to the ν_{C-O} in methanol. By referring to the coordination forms of methanol molecules in the Cu(II) with the 2-(2-hydroxy-3-methylphenyl)benzimidazole complex¹¹ and the weak bending vibration of O–H...O bridges around (1740 to 1720) cm⁻¹ in the IR spectra²⁶ of the Co(II) and Zn(II) with HL complexes, the methanol molecule in the Co(II) or Zn(II) complexes is hydrogen-bonded to the O atom of HL rather than coordinated to the metal center.

From these results, it can be concluded that the HL is coordinated to the metal ions via the phenolate oxygen and the imidazole nitrogen atoms, and the proposed structures of complexes is depicted in Figure 3.

3.2. Thermal Decomposition of M^{II}L₂·CH₃OH (M = Co, Zn) and M^{II}L₂ (M = Ni, Cu). For the complex Co^{II}L₂·CH₃OH, the TG curve (Figure 4) shows three main steps corresponding to the loss of one CH₃OH molecule (calcd 6.28 %, found 6.24 %), then to the loss of one ligand molecule, and finally to the slow decomposition process to give the metal oxide (calcd 15.85 %, found 16.76 %). The DSC curve (Figure 5) shows an endothermic peak related to the CH₃OH loss at 130 °C and then one big exothermic peak to give the metal oxide.

For the complex Zn^{II}L₂·CH₃OH, the TG curve (Figure 4) shows the first step is the loss of one CH₃OH molecule (calcd 6.21 %, found 6.27 %), followed by the loss of one ligand molecule that contains two steps, and then to the decomposition to give the metal oxide (calcd 15.72 %, found 16.61 %). In the DSC curve (Figure 5), the endothermic process appears due to the loss of CH₃OH and is followed by two exothermic peaks, and around 300 °C decomposition starts, giving ZnO.

In contrast with the former complexes, the TG curves of complexes NiL₂ and CuL₂ are quite simple, from the starting of decomposition at 300 °C to give the final metal oxide (for NiL₂: calcd 15.67 %, found 15.83 %; for CuL₂: calcd 16.51 %, found 17.45 %). There are two poorly resolved processes. According to this, the DSC curves (Figure 5) show a big exothermic peak.

The four complexes show two general formulas M^{II}L₂·CH₃OH (M = Co, Zn) and M^{II}L₂ (M = Ni, Cu). For the Co(II) and Zn(II) complexes, the fact that the temperature of losing one methanol molecule is not high (~130 °C) confirms that the methanol molecule does not coordinate to the metal ions. These two complexes are stable between (160 and 300) °C. The Ni and Cu complexes are stable up to around 400 °C. All of these four

Table 2. Color, Molar Conductance, and Elemental Analysis of the Complexes

compounds	color	Λ _m	calcd (found)/%			
		S·cm ² ·mol ⁻¹	C	H	N	M
Co(HL) ₂ ·CH ₃ OH	pink	1.24	63.66 (63.38)	4.35 (4.23)	11.00 (10.86)	11.59 (11.72)
Zn(HL) ₂ ·CH ₃ OH	white	1.05	62.68 (62.71)	4.30 (4.26)	10.86 (10.77)	12.61 (13.28)
Ni(HL) ₂	pale yellow	0.385	65.72 (65.31)	3.82 (3.61)	11.79 (11.46)	12.03 (11.85)
Cu(HL) ₂	brown	0.625	64.78 (64.59)	3.76 (3.69)	11.31 (11.31)	13.28 (12.95)

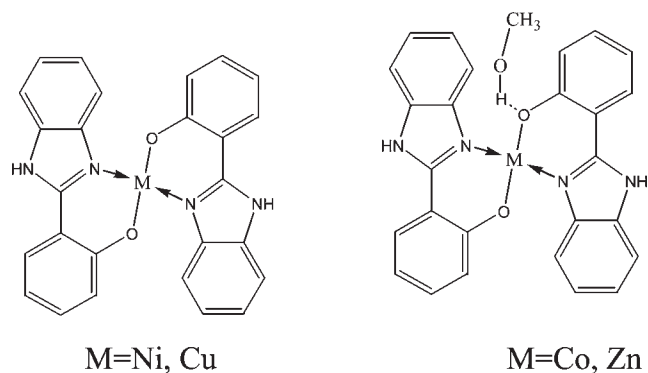


Figure 3. Proposed coordinated modes for the metal complexes with HPBL.

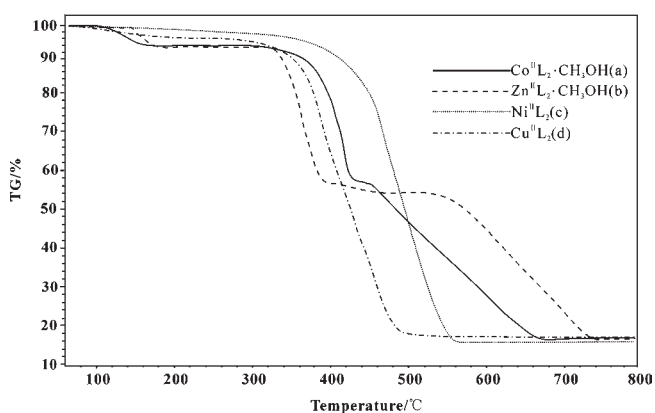


Figure 4. TG curve of $\text{Co}^{\text{II}}\text{L}_2 \cdot \text{CH}_3\text{OH}$ (a), $\text{Zn}^{\text{II}}\text{L}_2 \cdot \text{CH}_3\text{OH}$ (b), $\text{Ni}^{\text{II}}\text{L}_2$ (c), and $\text{Cu}^{\text{II}}\text{L}_2$ (d). Heating rate: $10\text{ }^\circ\text{C} \cdot \text{min}^{-1}$, nitrogen flow at a $30\text{ mL} \cdot \text{min}^{-1}$ rate.

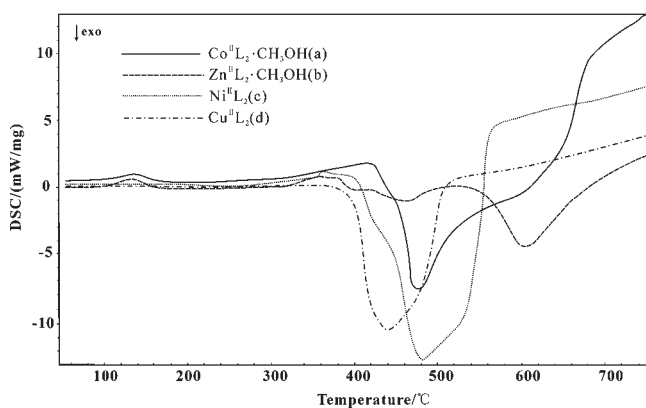


Figure 5. DSC curves of $\text{Co}^{\text{II}}\text{L}_2 \cdot \text{CH}_3\text{OH}$ (a), $\text{Zn}^{\text{II}}\text{L}_2 \cdot \text{CH}_3\text{OH}$ (b), $\text{Ni}^{\text{II}}\text{L}_2$ (c), and $\text{Cu}^{\text{II}}\text{L}_2$ (d). Heating rate: $10\text{ }^\circ\text{C} \cdot \text{min}^{-1}$, nitrogen flow at a $30\text{ mL} \cdot \text{min}^{-1}$ rate.

complexes have good stability except losing the methanol molecule, and the Ni complex shows the best thermal stability. The good thermal stability is attributed to the formed six-membered ring with the metal ions (Figure 3) and the strong coordinated bond between HL and metal ions.

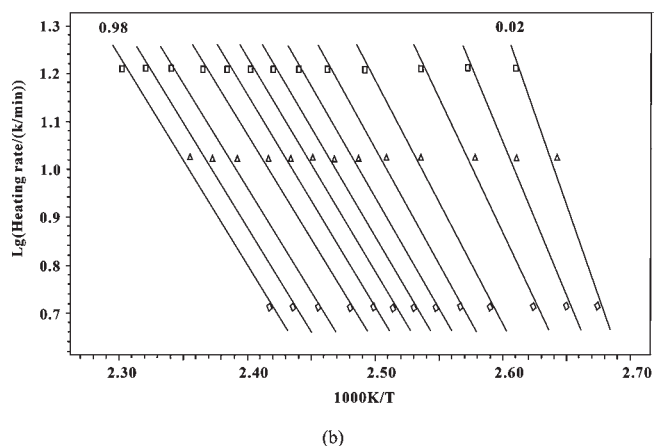
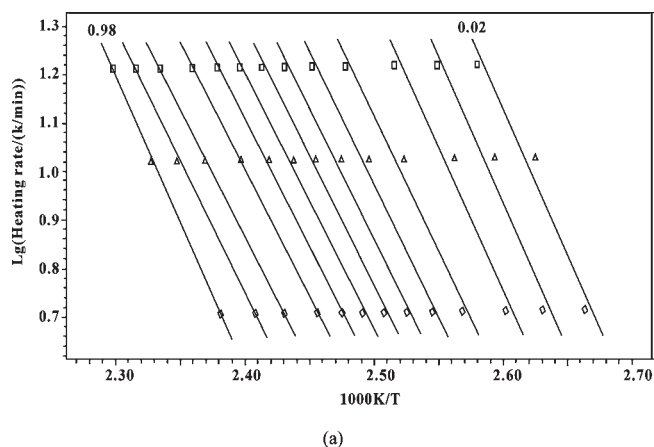


Figure 6. Isoconversional plots for the first-stage thermal decomposition of $\text{Co}^{\text{II}}\text{L}_2 \cdot \text{CH}_3\text{OH}$ (a) and $\text{Zn}^{\text{II}}\text{L}_2 \cdot \text{CH}_3\text{OH}$ (b).

Table 3. Activation Energy Values of $\text{Co}^{\text{II}}\text{L}_2 \cdot \text{CH}_3\text{OH}$ (a) and $\text{Zn}^{\text{II}}\text{L}_2 \cdot \text{CH}_3\text{OH}$ (b) Obtained from the Kinetic Analysis of the Isoconversional Lines of (Figure 5) by Means of Equation 6

a		b	
α	$E/\text{kJ} \cdot \text{mol}^{-1}$	α	$E/\text{kJ} \cdot \text{mol}^{-1}$
0.02	106.4	0.02	137.5
0.05	111.9	0.05	106.6
0.10	105.1	0.10	104.8
0.20	104.9	0.20	91.8
0.30	99.6	0.30	84.1
0.40	100.7	0.40	82.9
0.50	99.6	0.50	80.9
0.60	98.6	0.60	79.4
0.70	98.5	0.70	78.3
0.80	97.5	0.80	77.4
0.90	97.8	0.90	77.2
0.95	104.5	0.95	75.8
0.98	113.1	0.98	76.5

The area of the endothermic peak in the DSC (Figure 5) for the loss of one methanol molecule from the complexes $\text{Co}^{\text{II}}\text{L}_2 \cdot \text{CH}_3\text{OH}$ and $\text{Zn}^{\text{II}}\text{L}_2 \cdot \text{CH}_3\text{OH}$ was measured and calculated. The results are (48 and 60) $\text{kJ} \cdot \text{mol}^{-1}$, respectively. They have nearly

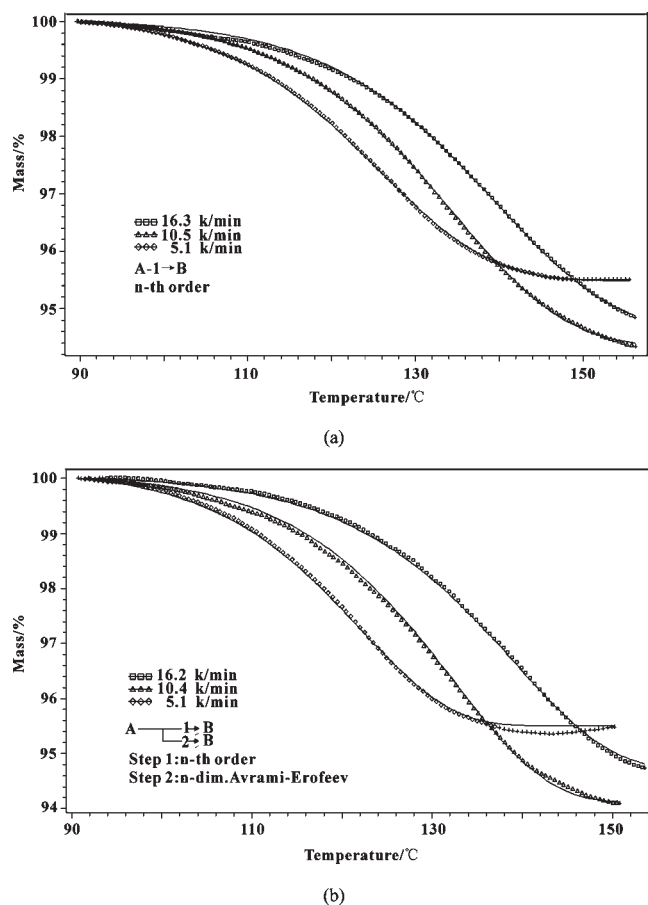


Figure 7. First step of TG curve of $\text{Co}^{\text{II}}\text{L}_2 \cdot \text{CH}_3\text{OH}$ (a) and $\text{Zn}^{\text{II}}\text{L}_2 \cdot \text{CH}_3\text{OH}$ (b) at the heating rate of (15, 10, and 5) $^\circ\text{C} \cdot \text{min}^{-1}$ as the best fit to mechanism functions. The solid lines are the fitted curve.

the same temperature for the endothermic peak, and the methanol molecule is proposed to have the same coordination form in the two complexes.

3.3. Kinetic Analysis of the First-Stage Decomposition of $\text{Co}^{\text{II}}\text{L}_2 \cdot \text{CH}_3\text{OH}$ and $\text{Zn}^{\text{II}}\text{L}_2 \cdot \text{CH}_3\text{OH}$. A nonisothermal kinetic analysis of the first-stage thermal decomposition was carried out using the data elaborated from the TG curves performed at different heating rates of (5, 10, and 15) $^\circ\text{C} \cdot \text{min}^{-1}$.

The isoconversion lines obtained in plotting $\log \beta$ versus the reciprocal of temperature (eq 6) in Figure 6, at the same degree of conversion, yield a series of activation energies, as shown in Table 3.

For the first-step decomposition of $\text{Co}^{\text{II}}\text{L}_2 \cdot \text{CH}_3\text{OH}$, from $\alpha = 0.2$ to $\alpha = 0.9$, the activation energy value is approximately invariable, about $99 \text{ kJ} \cdot \text{mol}^{-1}$, but at $\alpha < 0.2$ and $\alpha > 0.9$, there is little fluctuation ($5 \text{ kJ} \cdot \text{mol}^{-1} \sim 10 \text{ kJ} \cdot \text{mol}^{-1}$). The results apparently indicate a single reaction mechanism for the first-stage thermal decomposition of $\text{Co}^{\text{II}}\text{L}_2 \cdot \text{CH}_3\text{OH}$. However, for the first-step decomposition of $\text{Zn}^{\text{II}}\text{L}_2 \cdot \text{CH}_3\text{OH}$, in the process of losing a methanol molecule, the activation energy decreases monotonically from $137 \text{ kJ} \cdot \text{mol}^{-1}$ to $76 \text{ kJ} \cdot \text{mol}^{-1}$. The obtained dependencies probably indicate a multistep mechanism of the first-stage thermal decomposition of $\text{Zn}^{\text{II}}\text{L}_2 \cdot \text{CH}_3\text{OH}$.²⁷

Using the NETZSCH kinetic software, a multivariate nonlinear regression method has used to fit the kinetic curves. For the target stage of the TG curves of $\text{Co}^{\text{II}}\text{L}_2 \cdot \text{CH}_3\text{OH}$ and $\text{Zn}^{\text{II}}\text{L}_2 \cdot \text{CH}_3\text{OH}$, we

tried to use a single reaction mechanism to fit the curves. The results were different. To the first stage of $\text{Co}^{\text{II}}\text{L}_2 \cdot \text{CH}_3\text{OH}$, the model Fn ($n = 1.02$) was designated as the best fit (Figure 7a). The Arrhenius parameters were $E = 109.5 \text{ kJ} \cdot \text{mol}^{-1}$ and $\log A = 12.2 \text{ s}^{-1}$. But for the $\text{Zn}^{\text{II}}\text{L}_2 \cdot \text{CH}_3\text{OH}$, the fit result was not good. When we used a multireaction mechanism to fit, the result obtained was satisfactory (Figure 7b). There is a pair of parallel reactions. The mechanisms and Arrhenius parameters were Fn ($n = 0.87$), $E = 85.3 \text{ kJ} \cdot \text{mol}^{-1}$, $\log A = 8.6 \text{ s}^{-1}$, and An ($n = 1.79$), $E = 83.7 \text{ kJ} \cdot \text{mol}^{-1}$, $\log A = 8.5 \text{ s}^{-1}$, respectively. Using the ASTM E698 method, the Arrhenius parameters obtained are $E = 106.1 \text{ kJ} \cdot \text{mol}^{-1}$, $\log A = 11.5 \text{ s}^{-1}$ for the first-step decomposition of $\text{Co}^{\text{II}}\text{L}_2 \cdot \text{CH}_3\text{OH}$ and $E = 80.9 \text{ kJ} \cdot \text{mol}^{-1}$, $\log A = 8.2 \text{ s}^{-1}$ for the first-step decomposition of $\text{Zn}^{\text{II}}\text{L}_2 \cdot \text{CH}_3\text{OH}$. By comparing with the former two methods, the resulting predictions appear to confirm the kinetic scheme for the first-step decomposition of $\text{Co}^{\text{II}}\text{L}_2 \cdot \text{CH}_3\text{OH}$, but it cannot disclose the activation energy variations that may accompany the complex (e.g., multistep) kinetics of the first-step decomposition of $\text{Zn}^{\text{II}}\text{L}_2 \cdot \text{CH}_3\text{OH}$.

The loss of one methanol molecule reaction of the two complexes which have the same coordination form undergoes different reaction mechanisms may be attributed to the different center atom.

4. SUMMARY

The complexes $\text{M}^{\text{II}}\text{L}_2 \cdot \text{CH}_3\text{OH}$ ($\text{M} = \text{Co}, \text{Zn}$) and $\text{M}^{\text{II}}\text{L}_2$ ($\text{M} = \text{Ni}, \text{Cu}$) were prepared and characterized with HL as the ligand. These complexes showed good thermal stability around $300 \text{ }^\circ\text{C}$ except that a methanol molecule was lost in $\text{Co}(\text{II})$ and $\text{Zn}(\text{II})$ complexes, indicating strong coordinated bonds between the metal ion and ligand. The methanol molecule has a similar environment in the $\text{Co}(\text{II})$ and $\text{Zn}(\text{II})$ complexes due to them having almost the same temperature of endothermic peak. The nonisothermal kinetic analysis of the first-stage thermal decomposition of $\text{Co}(\text{II})$ and $\text{Zn}(\text{II})$ complexes showed a single reaction mechanism for the first-stage thermal decomposition of $\text{Co}^{\text{II}}\text{L}_2 \cdot \text{CH}_3\text{OH}$ but a multistep mechanism of the first-stage thermal decomposition of $\text{Zn}^{\text{II}}\text{L}_2 \cdot \text{CH}_3\text{OH}$.

■ AUTHOR INFORMATION

Corresponding Author

*Fax: 00 86 29 88303798. Tel.: 0086 29 88302604. E-mail address: junli@nwu.edu.cn.

Funding Sources

We are very grateful for the financial support from the National Nature Science funds (20971103) and the International Cooperation Project of Shaanxi Province (2008KW-33).

■ REFERENCES

- (1) Lei, Y.-J.; Ouyang, J.; Zhang, Y.-L.; Ding, M. Synthesis of 2-(1H-Benzo [d]imidazol-2-yl)phenyl Phosphate as a Fluorescent Probe for Determination of ALP. *Chin. J. Chem.* **2009**, *27*, 2413–2417.
- (2) Acuna, A. U.; Amat, F.; Catalan, J.; Costela, A.; Figuera, J. M.; Munoz, J. M. Pulsed Liquid Lasers from Proton Transfer in the Excited State. *Chem. Phys. Lett.* **1986**, *132*, 567–569.
- (3) Roberts, E. L.; Dey, J.; Warner, I. M. Excited-State Intramolecular Proton Transfer of 2-(2'-Hydroxyphenyl)benzimidazole in Cyclodextrins and Binary Solvent Mixtures. *J. Phys. Chem. A* **1997**, *101*, 5296–5301.

- (4) Shaikh, M.; Choudhury, S. D.; Mohanty, J.; Bhasikuttan, A. C.; Nau, W. M.; Pal, H. Modulation of Excited-State Proton Transfer of 2-(2'-Hydroxyphenyl) benzimidazole in a Macrocyclic Cucurbit[7]uril Host Cavity: Dual Emission Behavior and pK(a) Shift. *Chem.—Eur. J.* **2009**, *15*, 12362–12370.
- (5) Tsai, H. H. G.; Sun, H. L. S.; Tan, C. J. TD-DFT Study of the Excited-State Potential Energy Surfaces of 2-(2'-Hydroxyphenyl)benzimidazole and its Amino Derivatives. *J. Phys. Chem. A* **2010**, *114*, 4065–4079.
- (6) Iglesias, R. S.; Goncalves, P. F. B.; Livott, P. R. Semi-Empirical Study of a Set of 2-(2'-Hydroxyphenyl)Benzazoles Using the Polarizable Continuum Model. *Chem. Phys. Lett.* **2000**, *327*, 23–28.
- (7) Holler, M. G.; Campo, L. F.; Brandelli, A. D.; Stefani, V. Synthesis and Spectroscopic Characterisation of 2-(2'-Hydroxyphenyl)benzazole Isothiocyanates as New Fluorescent Probes for Proteins. *J. Photochem. Photobiol., A* **2002**, *149*, 217–225.
- (8) Fellah, F. Z. C.; Costes, J. P.; Duhayon, C.; Daran, J. C.; Tuchagues, J. P. Mononuclear Cu and dinuclear Cu-Ln complexes of benzimidazole based ligands including N and O donors: Syntheses, characterization, X-ray molecular structures and magnetic properties. *Polyhedron* **2010**, *29*, 2111–2119.
- (9) Chang, H.; Fu, M.; Zhao, X.-J.; Yang, E.-C. Four benzimidazole-based ZnII/CdII polymers extended by aromatic polycarboxylate coligands: synthesis, structure, and luminescence. *J. Coord. Chem.* **2010**, *63*, 3551–3564.
- (10) Tong, Y.-P.; Zheng, S.-L.; Chen, X.-M. Syntheses, Structures, Photoluminescence and Theoretical Studies of Two Zn(II) Complexes with Substituted 2-(2-Hydroxyphenyl)-benzimidazoles. *Eur. J. Inorg. Chem.* **2005**, 3734–3741.
- (11) Crane, J. D.; Hughes, R.; Sinn, E. Preparation of the Complexes $MnLe \cdot 2CH_3OH$ ($M = Co, Ni, Cu, Zn$) of the Bidentate Ligand 2-(2'-Hydroxy-3'-Methylphenyl) Benzimidazole (HL) and the Molecular Structure of $CuUL_2 \cdot 2CH_3OH$. *Inorg. Chim. Acta* **1995**, *237*, 181–185.
- (12) Crane, J. D.; Sinn, E.; Tann, B. Homoleptic Cobalt(II) and Cobalt(III) Complexes of the Sterically Demanding Bidentate Ligand N-Ethyl-2-(29-hydroxy-39-methylphenyl)Benzimidazole. *Polyhedron* **1999**, *18*, 1527–1532.
- (13) Tong, Y.-P.; Zheng, S.-L.; Chen, X.-M. Syntheses, Structures, Photoluminescence, and Theoretical Studies of a Class of Beryllium(II) Compounds of Aromatic N,O-Chelate Ligands. *Inorg. Chem.* **2005**, *44*, 4270–4275.
- (14) Xi, Y.; Li, J.; Zhang, F.-X. Bis[2-(1H-benzimidazol-2-yl)phenolato]Copper(II) Dimethylformamide Disolvate. *Acta Crystallogr.* **2005**, *E61*, m1953–m1954.
- (15) Xi, Y.; Jiang, M.; Li, J.; Wang, C.; Yan, J.-F.; Zhang, F.-X. Synthesis, Crystal Structure and Thermal Decomposition of a Novel Trinuclear Nickel Complex $[Ni_3(C_{13}H_9N_2O)_5(CH_3OH)(CH_3-CH_2OH)]$. *Acta Chim. Sin.* **2006**, *64*, 1183–1188.
- (16) Duan, M.-Y.; Li, J.; Xi, Y.; Lü, X.-F.; Liu, J.-Z.; Mele, G.; Zhang, F.-X. Synthesis and Characterization of Binuclear Manganese(IV,IV) and Mononuclear Cobalt(II) Complexes Based on 2-(2-hydroxyphenyl)-1H-benzimidazole. *J. Coord. Chem.* **2010**, *63*, 90–98.
- (17) Doyle, C. D. Kinetic analysis of thermogravimetric data. *J. Appl. Polym. Sci.* **1961**, *15*, 285–292.
- (18) Vyazovkin, S.; Dollimore, D. J. Linear and Nonlinear Procedures in Isoconversional Computations of the Activation Energy of Nonisothermal Reactions in Solids. *Chem. Inf. Comput. Sci.* **1996**, *36*, 42–45.
- (19) Ozawa, T. A. New Method of Analyzing Thermogravimetric Data. *Bull. Chem. Soc. Jpn.* **1965**, *38*, 1881–1886.
- (20) Flynn, J. H.; Wall, L. A. A quick, direct method for the determination of activation energy from thermogravimetric data. *J. Polym. Sci., Part B: Polym. Lett.* **1966**, *4*, 323–328.
- (21) *Standard Test Method for Arrhenius Kinetic Constants for Thermally Unstable Materials*, ANSI/ASTM E698-79; ASTM: Philadelphia, 1979.
- (22) Kissinger, H. E. Reaction Kinetics in Differential Thermal Analysis. *Anal. Chem.* **1957**, *29*, 1702–1706.
- (23) Vyazovkin, S.; Wight, C. A. Model-free and model-fitting approaches to kinetic analysis of isothermal and nonisothermal data. *Thermochim. Acta* **1999**, *340–341*, 53–68.
- (24) Geary, W. J. Use of Conductivity Measurements in Organic Solvents for the Characterization of Coordination Compounds. *Coord. Chem. Rev.* **1971**, *7*, 81–122.
- (25) Teyssie, P.; Carette, J. J. Physicochemical Properties of Coordinating Compounds-III; Infra-Red Spectra of N-Salicylidenealkylamines and Their Chelates. *Spectrochim. Acta* **1963**, *19*, 1407–1423.
- (26) Gül, A.; Bekaroglu, Ö. Syntheses of N,N'-bis(4'-benzo[15-crown-5]) Diaminoglyoxime and its Complexes with Copper(II), Nickel(II), Cobalt(II), Palladium(II), Platinum(II), and Uranyl(VI). *J. Chem. Soc., Dalton Trans.* **1983**, *12*, 2537–2541.
- (27) Vyazovkin, S. Kinetic concepts of thermally stimulated reactions in solids: a view from a historical perspective. *Int. Rev. Phys. Chem.* **2000**, *19*, 45–60.